Journal: International Journal of Healthcare Information Systems and Informatics

Topic: Extraction Gap – Space + Time Dimension Gap

Bridging the Feature Gaps for Retrieval of Multi-dimensional Images

Jinman Kim[1,2], Weidong Cai[1,2], and Dagan Feng[1,2]

1. Biomedical and Multimedia Information Technology (BMIT) Research Group, School of Information Technologies, University of Sydney, Australia

2 Centre for Multimedia Signal Processing, Department of Electronic and Information Engineering, Hong Kong Polytechnic University, Hong Kong

Abstract

Content-based image retrieval (CBIR) refers to the use of visual features of images for retrieval from an image database, and has become an attractive approach to managing medical image databases. However, existing CBIR systems are typically designed for 2D single-modality imaging, and are restricted when multi-dimensional imaging modalities are considered. With the advances in imaging scanners, image complexity and magnitude have also rapidly expanded in both the temporal (time) and spatial (space) dimensions. A biomedical imaging modality such as dynamic positron emission tomography (PET) provides physiological functions of the human body acquired in three-dimension (3D) volumes over multiple time sequences. More recently, dual-modality imaging scanners are now sequentially acquiring functional (PET) and anatomical (CT) images that are co-aligned and complimentary. These multi-dimensional imaging modalities are requiring new innovative techniques for content-based retrieval to fully utilize the massive amount of information in a meaningful and practical manner. This manuscript summarizes research in bridging the feature gap for retrieval of multi-dimensional biomedical images. We focus on studies where the feature extraction and retrieval were performed using information available in the image's multi-dimensional data spaces. Applications of multi-dimensional CBIR will be exemplified with our ongoing studies with 4D dynamic PET and dual-modal PET/CT images.

Keywords: Multi-dimensional imaging, Space dimension, Time dimension, content-based image retrieval, functional imaging, PET/CT, dynamic PET

I. INTRODUCTION

Advances in digital biomedical imaging are enabling unprecedented understanding of structures, functions, and pathologies of the human body, thus providing powerful tools for patient diagnosis, treatment planning, medical references, and training [1]. Together with the adaptation of integrated databases, i.e., picture archiving and communication systems (PACS), techniques for efficient image retrieval and management are becoming ever more important. The volume of medical data online in PACS often exceeds several terabytes, due to increase in the number of diverse clinical exams performed and to the large range of biomedical imaging modalities. In current medical image databases, images are indexed and retrieved mainly by text-based keywords that are classified by human experts often with standard medical terminology. However, these approaches are not able to sufficiently describe the rich visual properties or features of the image content and therefore impose significant limitations on image retrieval capabilities [3, 4].

Content-based image retrieval (CBIR) refers to the use of visual attributes of the image for retrieval from an image database, and has become an attractive technique in managing large medical image databases [4-6]. Recent years has resulted in the introduction of many domain-specific CBIR solutions for a large array of medical imaging modalities [5-7], such as for high-resolution lung CT [5] and microcalcification from mammography [8], as well as methods to automatically categorize medical images as in [9]. However, the majority of existing CBIR systems are typically designed for two-dimensional (2D) slices, even though the images acquired were multi-dimensional, and are thus not taking full advantage of the information available in all the image dimensions.

Modern biomedical imaging scanners have the capability to acquire images in multiple dimensions – 3D spatial images (space) such as with computed tomography (CT), and magnetic resonance imaging (MRI); in dynamic temporal sequences (time), i.e., dynamic positron emission tomography (PET), functional MRI, and ultrasound; as well as in combined dual-modality imaging e.g., sequentially acquired and co-aligned PET/CT. Because dual-modality imaging is the combination of two full 3D image volumes, it can be considered as four-dimensional (4D), where the PET volume with lower resolution is resampled to that of the higher resolution CT. These multi-dimensional biomedical imaging modalities are requiring new approaches to fully utilize all the information within the image data for content-based retrieval, while at the same time introducing new challenges and opportunities for CBIR research and development. There have been numerous researches that investigated the use of the entire range of information within the multi-dimensional images for feature extraction, representation, and retrieval.

In a study by Shyu et al. [5], delineations of pathology bearing regions were manually defined by physicians, along with a set of anatomical landmarks on a *key frame* – a single image slice selected from an image stack. Such a *key frame* was used to extract features that represented an entire image volume for content-based retrieval of high resolution CT (lung) image. Together with the *key frames*, other contiguous images which carry important diagnostic meaning, i.e., information regarding the 3D extends and shape of the pathology were also indexed into the database.

Liu et al. [10] introduced a content-based retrieval technique based on 3D ideal midsaggital plane (iMSP) features for retrieving 3D CT neuroimages of hemorrhage (blood), bland infarct (stroke), and normal brain structures. A basic observation from neuroradiologic imaging is that normal human brains exhibit an approximate bilateral symmetry that is often absent in pathological brains. Given this observation, a symmetry detector was first constructed to automatically extract an iMSP – a virtual geometric plane about which the 3D anatomical structure captured in a brain image presents maximum bilateral symmetry [11]. Using the iMSP for pathological brain alignment for comparison, asymmetrical regions were detected automatically as possible lesions (e.g., bleeds, stroke, and tumors). A set of relatively simple and computationally inexpensive statistical image features were then collected to quantify and capture the statistical distribution differences of various brain asymmetries. For each image, a feature vector with 48 image features was constructed and used in the retrieval of similar pathological brain images.

Guimond et al. [12] introduced the use of a user-defined volume of interest (VOI) for the content-based retrieval of pathological 3D brain MRI images. The VOI was defined as a subdivision of the image volume. The retrieval process was performed using a density-based registration algorithm (global/local affine followed by a free-form transformation) to identify the best match between the user-defined VOI and images in the database, and the correlation between the compared images were used as a measure for morphological differences

In a recent study, Kontos and Megalooikonomou [13] proposed a method for characterizing spatial region data using concentric spheres in 3D (or circles in 2D) radiating out of a region's center of mass, thus segmenting data into regions of interests (ROIs) of homogeneous properties. In this process, *k*-dimensional feature vectors were derived from the ROIs to capture the structural and internal volume properties. This approach was a general solution and its capabilities were exemplified with the extraction and retrieval of features derived from the ROIs segmentation of 3D clinical fMRI brain activation contrast maps.

A multimodality database for content-based image management, navigation, and retrieval for temporal lobe epilepsy was proposed by Siadat et al. [14]. Here, a segmentation based on deformable model was used to segment out and label the hippocampus structures from 3D T1 MRI images, which were then subject to region-based feature extraction and subsequent retrieval. The multimodality aspect of this study was the ability to overlay the segmented hippocampus structures on images of different modalities (i.e., SPECT, T2 MRI etc) of the same patient. In this process, the segmented T1 MRI was used to spatially align the other imaging modalities based on image registration.

In this manuscript, summary and discussion on bridging the feature gaps for the retrieval of multi-dimensional biomedical images will be presented based on our ongoing research on CBIR for multi-dimensional functional imaging of dynamic PET and dual-modal PET/CT [2, 7, 15, 16]. Developed prototype systems will be use to demonstrate the necessities and advantages for feature extraction and retrieval to be performed on multi-dimensional image data space that are available in modern biomedical images. A CBIR system that uses tissue activities derived from the temporal (time) dimension of dynamic PET images, together with visual features that were extracted from the 3D spatial (space) dimension will be summarized. This will be followed by an introduction to dual-modality PET/CT images and their application to CBIR, presenting the unique characteristics and challenges with multi-dimensional information in the dual-modality imaging. Finally, concluding remarks on multi-dimensional CBIR will be discussed.

II. Physiological and Functional Retrieval of 4D dynamic PET images

The functional imaging modality of PET allows *in vivo* studies of physiological processes [17]. To estimate physiological function, dynamic PET images are acquired in 4D (three spatial and one temporal dimensions), by quantifying the radiotracer distribution at pre-determined sampling times. From these data, a physiological tissue time-activity curve (TTAC) can be extracted for each voxel and the physiological parameter value for that voxel can then be calculated by the application of a tracer kinetic model to the TTAC. Although physiological parameter estimation can be performed from the kinetic modeling of individual voxels, estimation based on segmented regions comprising functionally and structurally related voxels can be of considerable benefit in a variety of neuro-imaging applications [18-20]. For instance, the image classification based on the characteristics of the TTAC in dynamic PET images is often facilitated by using regional parameters from the segmentation definition [20]. Moreover, dynamic PET image segmentation enables region-based feature extraction and retrieval, for example, search for previous diagnosis and treatment results for cases with a cerebral tumor near the cerebellum of the brain.

Cai et al. [15] proposed a CBIR system for functional 4D dynamic PET images of the human brain, where the segmented clusters of TTACs from the temporal domain were used to measure the functional similarity for retrieval. In this process, a novel approach to incorporating time dimension to CBIR was introduced. Our further research in [7] extends this work with dynamic PET image retrieval with the addition of spatial features derived from the space dimensions. Visual and functional features were extracted from segmented VOIs, which allowed the users to formulate multi-dimensional region-based queries for content-based retrieval. Fig. 1 illustrates the overall system block diagram of the content-based retrieval of dynamic PET images.

Volume-of-Interest (VOI) Feature Extraction

Feature Extraction

As an initial stage for feature extraction, voxels in the dynamic PET mages were automatically segmented with modified fuzzy c-means cluster analysis [21] into cluster groups, where the voxel's kinetic behaviors in the form of TTACs were used in the similarity measure. In this process, a fuzzy logic algorithm assigns probabilistic weights to every voxel representing the likelihood that it is a member of each cluster. From the cluster analysis results, region growing segmentation [22] was applied to the voxels in each cluster to construct the VOIs. After region growing, an erosion filter was applied to remove weakly connected voxels in the VOIs. Multiple VOIs may be formed from each cluster and for VOIs comprising of less than 100 voxels were considered insignificant and discarded.

From each identified VOIs, functional and visual features were extracted and indexed. As functional features, two physiological parameters were extracted. First, the average of the TTACs in the VOI was calculated. Secondly, the local cerebral metabolic rate of glucose [23] corresponding to the glucose consumption and energy requirement of functional components was estimated with a weighted non-linear least square algorithm [24]. To extract the visual features, PET images were initially transformed into a standard atlas using anatomical standardization procedure of the 3D stereotactic surface projection transformation in the Neurostat package [25-27], which deforms the image into a standard stereotactic atlas by linear scaling of the image to correct individual brain sizes and nonlinear warping to minimize regional anatomical variations. After the transformation, for every VOI, the centroid moment of the VOI (3D co-ordinate) was calculated as the spatial location and its number of voxels as volume. In addition, conventional textual features were extracted from the PET image headers which included information such as patient ID, name, gender, age, weight, patient history, and pathological results.

Feature Similarity Measures

To retrieve the VOIs, individual features maybe used as queries and the feature database then returns the VOIs in the order of similarity. The similarity measure of the features is calculated as absolute differences between two values or between two curves (i.e., TTACs). Fig. 2 shows the graphical user interface of the query components which was designed to enable user query to be defined in multi-dimensions. With the use of multi-dimensional image features, an intuitive and simple user interface was necessary to minimize the complexities and difficulties in formulating a query for dynamic PET images. Query interface design is an important and a general problem associated with "query gap", which when implemented correctly, can enable greater retrieval capabilities and usability. In this study, four individual query entry windows were designed which corresponds to four different query options – separating the complexity in multi-dimensional feature selections into smaller and independent components. With the "Query by functional and physiological features" presented in Fig. 2(a), the user can manually draw/input the TTAC feature curve, or select from a list of predefined sample

TTACs. The "Query by VOI visual features" is illustrated in Fig. 2(b), where a Zubal phantom [28] which consists of labeled anatomical structures was transformed into the standard atlas as with PET images, thus acting as a labeled reference image. The user can navigate (rotation, scaling, and translation) in the 3D orthogonal viewing space during the selection of a location feature which can be either by selecting a point on the Zubal phantom, or by selecting from the labeled Zubal structures. The volume of the VOI can also be set numerically which works independently to the location feature. The "Query by textual attribute features" shown in Fig. 2(c) allow the users to input key words as in conventional SQL query. In addition, the primary query features of TTAC, volume, and location, can be combined into a single query by assigning different weights (priority) to these features as in "Query by combined features" illustrated in Fig. 2(d). For every exclusive VOI retrieved from all M queries, rank of a combined query, R_{CQ}, was calculated based on the summation of the ranks from the individual queries according to

$$R_{CQ}(VOI_j) = \sum_{i}^{M} \frac{R(VOI_j, Q_i)}{R_T} w_i \qquad (1)$$

where VOI_j was the j^{th} exclusive VOI, and the R_T is the maximum number of returned VOI results which was common among all M queries ($Q_1, Q_2, \ldots, Q_N$), $R(VOI_j, Q_i)$ was the rank of the j^{th} VOI from the i^{th} query, Q_i, and w_i (sum to 100%) was the user defined weight assigned to Q_i. The returned VOIs from the combined queries were then ranked based on descending R_{CQ} measures. Textual patient attributes may also be combined without the weighting function.

Experimental Results

The content-based retrieval of dynamic PET images was demonstrated with the construction of a feature index database consisting of more than 300 unique and independent VOIs segmented from 13 individual patient studies of dynamic *[18F]2-fluoro-deoxy-glucose* (FDG) brain PET images (SIEMENS ECAT 951R scanner). These studies included two tumor cases, three normal cases, and eight other neurological cases. Although only a small database samples were indexed, all the images were acquired from the same scanner with identical imaging procedures (reconstruction algorithm, voxel dimension, spatial resolution, quantification, etc.). Therefore, many of the potential differences in the feature computation that different image acquisition introduces are avoided, e.g., filter back projection (FBP) reconstruction used in our image set will result in different VOIs segmentation definition (thus also the subsequent VOI-based features), when an alternate reconstruction algorithm such as optimized subset expectation maximization (OSEM) reconstruction is used.

Fig. 3 demonstrates the retrieval system. Each thumbnail result (Fig. 3(a)-(d)) can be individually navigated in orthogonal planes. The similarity indices from the retrieved VOIs are presented below the images. Any of the retrieved images can be enlarged and the VOI surface rendered (Fig. 3(e)). In this example, the combination query was formulated to search for dynamic PET images having similar functional behavior and apparent size in a malignant brain tumor cases of relatively large volume localized within the upper brain section. Three features were used to formulate the query – VOI location (x:65 y:97 z:30 where the atlas's image dimension is x:128 y:128 z:60) and volume (1000 voxels) as the spatial features, and TTAC (plotted in Fig. 2(a)) as the functional feature.

Feature weightings were set as 50:30:20, respectively of TTAC, location, and volume features. As expected, the highest ranked result was of a patient study with a known prominent tumor (Fig. 3(a) and enlarged in Fig. 3(e)), followed by another patient study with tumor as the 2nd ranked result (Fig. 3(b)). The result suggests that the query successfully identified VOIs with most similar user-defined features which were in agreement with the similarity indices. The similarity indices for all the features has been normalized between the values of [0,1] where 1 represents identical pair.

In order to test the benefits in incorporating spatial feature together with functional feature, a query was formulated to search for “right thalamus” VOIs. When only the functional TTAC feature which approximates a pattern found in *grey matter* was used for the query, although the thalamus VOIs were retrieved, both the left and right thalamus was retrieved and they were ranked lower than other non-thalamus VOIs that also shared similar TTACs. The results were markedly improved when “right thalamus” selected from the labeled structures in the Zubal phantom was further included (50% TTAC and 50% location features) in the query, retrieving VOIs of the right thalamus as the highest ranked results. From utilizing the spatial property of the PET image as the location feature, VOIs correlating to the user-selected structure were identified which may have not been possible from using the functional feature alone. Please refer to our previous work in [7] for additional examples and explanation of the retrieval results.

III. Dual-modality Biomedical Image Retrieval (4D space)

Dual-modality imaging that combines anatomical and functional images have considerably improved tumor staging and treatment planning [29]. PET/CT can, for example, detect tumor invasion into adjacent tissues, as well as provide precise localization of lesions, even when no morphological changes are identified by CT [30]. In lung cancer staging and therapy planning, determination of a tumor's size, its invasion into adjacent structures, mediastinal node status, and the detection of distant metastases are of great importance [30]. Single positron emission computed tomography (SPECT)/CT has also been recently released [31] which provides alternate functional image acquisition, with the expectation of PET/MR within the next few years [32]. Prototype of PET/MR has already demonstrated capabilities that may have a significant impact in patient care by enabling the sequential acquisition of high detailed soft tissue contrast combined with functional PET.

With these dual-modality scanners acquiring massive and complex images that occupy multi-dimensional spatial space, innovations in content-based retrieval are required to fully utilize the unique characteristics and opportunities arising from these next-generation imaging modalities. In our recent study [16], we investigated the potential of content-based approach to retrieving dual-modality PET/CT images. Lung cancer, which is the leading cause of tumor-related deaths in the world [29] has been used to exemplify the potential of application of CBIR for PET/CT.

PET/CT Feature Extraction and Retrieval

Features in PET/CT, that utilized the unique properties from co-aligned and complimentary information in anatomical CT and functional PET image pairs, were automatically extracted. Initially, anatomical lung structures from the CT image were segmented as *priors* based on automated approach in [33] consisting of adaptive thresholding, spatial region growing, airway/artifact removal, and finally lung separation and labeling. These segmented CT priors were then used to crop the co-aligned PET images. The cropping with the *prior* serves to remove structures that share similar pixel activity (intensity values), such as a heart structure, and hence simplifies the following fuzzy-c-means cluster analysis [21] for possible functional tumor identifications. Further details of PET/CT segmentation maybe found in [34]. The segmented regions from CT (lung structures) and PET (functional tumors) were used to derived region-based features including shape, size, and average pixel values, as well as the labelling of left/right lung structure in the CT. These features were indexed in a feature database together with conventional textual information from the PET/CT image header. The PET/CT retrieval in this dual-modal CBIR was performed by measuring the similarity of two regions based on the dice similarity coefficient (DSC) [35] which measures the spatial overlap between the query region A_{QU} and regions in the database A_{DB} defined as

$$DSC = 2\left|A_{QU} \cap A_{DB}\right| / \left|A_{QU}\right| + \left|A_{DB}\right| . \tag{2}$$

The *DSC* was in the range of [0,1], where 1 represents two areas of identical size and overlap. Although the feature regions were indexed in 3D, the similarity matching was performed using 2D regions, due to widely varying sizes and placement of the shapes within the lungs [16]. Nonetheless, this approach provided a good approximation of the tumor retrieval and was able to demonstrate the use of dual-modal features. Other conventional query options include searching by region size (pixel count of a region) and average pixel values, which were measured in absolute differences, as well as with the traditional keyword matching using SQL functions.

Experimental results

To investigate the PET/CT lung cancer retrieval possibilities, a database consisting of 10 individual patient studies of clinical high-resolution and whole-body (FDG) PET/CT (Siemens Biograph TruePoint 64 scanner) were used to extract the features. The database consisted of five known lung cancer and others of healthy lung cases. These PET and CT images were cropped and rescaled to equal dimensions of 256×256 pixels per imaging slice. For a typical whole-body study, the numbers of imaging slices were 350-450 slices, and the segmented lungs occupied in the range of 130-150 slices.

A query was formulated to search for all PET/CT studies that have a tumor structure of size 70-pixel residing on the right lung. This query requires the similarity matching of tumors based on size (pixel count) differences from the PET images, and then using the retrieved PET features to check if the tumor belongs in the left or right lung from its corresponding CT features. The results of this query are shown in Fig. 4, which have successfully retrieved all the right lung cancer studies (two in the database), sorted according to their region's size similarity to the query input. The option to select studies with number of tumors equals to one only returned (b), with (c) having two tumor regions. Further modification to this query to search for PET/CT studies based on a user-defined region (a), again resulted in only (b), since (c) didn't have any spatially overlapping pixels to (a). This demonstrates that the correct tumor shapes were retrieved based on functional similarity and that all these images were inside the right lung based on its anatomical counterpart. Other possible queries include searching by lung's size (in bounding box), or retrieval of right lung studies that includes tumor(s) of size less than the user-specified value.

The retrieved results are a set of volumetric PET/CT images. To represent this massive and complex image data, we used our previously developed dual-modality PET/CT image viewer shown in Fig. 5 that enables full interactive navigation of the data sets in three orthogonal views simultaneously (axial, saggital, and coronal), as well as the conventional image manipulation features (LUT, brightness/contrast, fusion ratio, etc) [36]. Because the retrieved data were accompanied with query parameters, these can be used to preset the volume data to automatically highlight the query-relevant sections from the dual-modal and full-body PET/CT images. This ability enabled immediate visualization of the parts of the image volume that were most relevant to the query. For both the PET/CT and dynamic PET images, these multi-dimensional images introduce tremendous challenges toward visualization of retrieved results in an efficient and practical manner for browsing through these large data. The ability to quickly grasp the important and relevant information from the retrieved images that are in multi-dimensions is a critical problem. In our experiments, the complexity and amount of time needed to navigate through the retrieved results were restricting the usability of our system. Our further studies will investigate this problem and incorporate automated visualization techniques [37] to simplify and represent the data in an intuitive and abstracted manner.

The CT segmentation algorithm when applied to clinical data sets were not always able to segment out only the lung structures, with parts of the lung nodules and airways not being fully removed. Furthermore, the separation of the lungs, at some cases, required multiple (up to 3) applications of an erosion filter which had the undesired effect of altering the lung shapes. In PET segmentation, due to the large variations in the pixel's glucose uptake activities (intensity values) from individual patients, the identification of the lesion clusters was not always correct. Out of the 5 lung cancer cases, one tumor cluster was manually corrected due to its extremely low activities (pixel values). This problem will be investigated with the use of standard uptake values (SUV) [38] which is expected to scale the pixel's values to a standard unit. These segmentation issues were expected from experimentation on clinical data sets. Even with these limitations, the segmented tumors and lung structures were clearly identifiable.

IV. CONCLUSION

Due to the rapid developments in biomedical imaging, modern biomedical imaging scanners are now able to acquire images of the human body in multiple dimensions and modalities, thus enabling never-before-possible diagnostic capabilities. The complexity and magnitude of these data provides unprecedented amount of information, which when translated into image features, has the potential to enable brand new capabilities in CBIR systems. Features to represent time dimension require unique approaches in order to capture the temporal information. In space dimension, 3D spatial information from multiple imaging modalities are presenting new challenges and potential for content-based retrieval.

The results from our previous studies demonstrated the application of multi-dimensional features for the content-based retrieval of dynamic PET and dual-modality PET/CT images, which can find potential applications in data management, such as for education, computer-aided diagnosis, and in statistical analysis. We are currently further developing and improving our system in all areas, including feature extraction, retrieval options, and better utilization of the massive amount of obtainable information in the multi-dimensional images. Our future work will address the currently known limitations and deploy our solution on a much larger database for quantitative assessment and broaden the use of different imaging modalities.

ACKNOWLEDGEMENT

This work was supported in part by the ARC and the Polytechnic University grants.

V. REFERENCES

[1] Feng, D., Siu, W.C., & Zhang, H.J. (2003). *Multimedia information retrieval and management – technological fundamentals and applications*. NY: Springer.

[2] Cai, W., Kim, J., & Feng, D. (2007). Content-based medical image retrieval. In D. Feng (Ed.), *Biomedical Information Technology* (pp. 83-113), San Diago: Elsevier Press.

[3] Lehmann, T.M., Güld, M.O., Thies, C., Fischer, B., Spitzer, K., Keysers, D., & Ney, H. (2004). Content-based image retrieval in medical applications. *Methods Inf. Med*., 43(4), 354-361.

[4] Müller, H., Michoux, N., Bandon, D., & Geissbuhler, A. (2004). A review of content-based image retrieval system in medical applications – clinical benefits and future directions. *Int. J. Med. Informatics*, 73, 1-23.

[5] Shyu, C., Brodley, C., Kak, A., Kosaka, A., Aisen, A., & Broderick, L. (1999). ASSERT: A physician-in-loop content-based image retrieval system for HRCT image databases. *Compt. Vision and Image Understanding*, 75, 111-132.

[6] Yu, S-N., Chiang, C-T., & Hsieh, C-C. (2005). A three-object model for the similarity searches of chest CT images. *Comp. Med. Imag. Graphics*, 29, 617-630.

[7] Kim, J., Cai, W., Feng, D., & Wu, H. (2006). A new way for multidimensional medical data management: volume of interest (VOI)-based retrieval of medical images with visual and functional features. *IEEE Trans. Info. Tech. Biomed*., 10(3), 598-607.

[8] El-Naqa, I., Yang, Y., Galatsanos, N.P., Nishikawa, R.M., & Wernick, M.N. (2004). A similarity learning approach to content-based image retrieval: application to

digital mammography. *IEEE Trans. Med. Imag.*, 23, 1233-1244.

[9] Lehmann, T.M., Guld, M.O., Deselaers, T., Keysers, D., Schubert, H., Spitzer, K., Ney, H., & Wein, B.B. (2005). Automatic categorization of medical images for content-based retrieval and data mining. *Elsevier Computerized Medical Imaging and Graphics*, 29, 143-155.

[10] Liu, Y., Lazar, N.A., Rothful, W.E., Dellaert, F., Moore, A., Schneider, J., & Kanade, T. (1998). Semantic-based biomedical image indexing and retrieval. *Trends and Advances in Content-based Access of Image and Video Libraries, in Conjunction with Int. Conf. Computer Vision*, 91-100.

[11] Liu, Y., Collins, R.T., & Rothfus, W.E. (2001). Robust midsaggital plane extraction from normal and pathological 3D neuroradiology images. *IEEE Trans. Med. Imag.*, 20(3), 175-192.

[12] Guimond, A., Subsol, G., & Thirion, J-P. (1997). Automatic MRI database exploration and applications. *Int. J. Patt. Recogn. Artific. Intell.*, 11, 1345–1365.

[13] Kontos, D., & Megalooikonomou, V. (2005). Fast and effective characterization for classification and similarity searches of 2D and 3D spatial region data. *Elsevier Pattern Recognition*, 38, 1831-1846.

[14] Siadat, M-R., Soltanian-Zadeh, H., Fotouhi, F., & Elisevich, K. (2005). Content-based image database system for epilepsy. *Elsevier Computer Methods and Programs in Biomedicine*, 79, 209-226.

[15] Cai, W., Feng, D., &Fulton, R. (2000). Content-based retrieval of dynamic PET functional images. *IEEE Trans. Info. Tech. Biomed.*, 4, 152-158.

[16] Kim, J., Constantinescu, L., Cai, W., & Feng, D. (2007). Content-based Dual-

Modality Biomedical Data Retrieval Using Co-Aligned Functional and Anatomical Features. *MICCAI workshop on Content-based Image Retrieval for Biomedical Image Archives*, 45-52.

[17] Feng, D., Ho, D., Lida, H., & Chen, K. (1997). Techniques for functional imaging. In. C.T. Leondes (Ed,), *Medical Imaging Systems Techniques and Applications: General Anatomy (pp. 85-145). Amsterdam: Gordan and Breach Science Publisher*.

[18] Montgomery, D.W.G., Amira, A., & Zaidi, H. (2007). Fully automated segmentation of oncological PET volumes using a combined multiscale and statistical model. *Med. Phys*., 34(2), 722-736.

[19] Liptrot, M., Adams, K.H., Martiny, L., Pinborg, L.H., Lonsdale, M.N., Olsen, N.V., Holm, S., Svarer, C., & Knudsen, G.M. (2004). Cluster analysis in kinetic modeling of the brain: a noninvasive alternative to arterial sampling. *Neuroimage*, 21, 483-493.

[20] Yap, J.T., Cunningham, V.J., Jones, T., Cooper, M., Chen, C-T., & Price, P. (1998). Classification of dynamic PET images using a priori kinetic factors. In R. Carson, M. Daube-Witherspoon & P. Herscovitch (Ed.), *Quantitative Functional Brain Imaging with PET,* San Diago: Academic Press.

[21] Bezdek, J. (1981). *Pattern recognition with fuzzy objective function algorithm*. Norwell: Kluwer Academic Publishers.

[22] Gonzalez R.C., & Woods, R.E. (2002). *Digital image processing*. NJ: *Prentice Hall*.

[23] Huang, S.C., Phelps, M.E., Hoffman, E.J., Sideris, K., Selin, C.J., & Kuhul, D.E. (1980). Non-invasive determination of local cerebral metabolic rate of glucose in man. *Am. J. Physiol*., 238, e69-e82.

[24] Feng, D., Ho, D., Chen, K., Wu, L-C., Wang, J-K., Liu, R-S., & Yeh, S-H. (1995). An evaluation of the algorithms for determining local cerebral metabolic rates of glucose using positron emission tomography dynamic data. *IEEE Trans. Med. Imag.*, 14, 697-710.

[25] Minoshima, S., Berger, K.L., Lee, K.S., & Mintun, M.A. (1992). An automated method for rotational correction and centering of three-dimensional functional brain images. *J. Nucl. Med.*, 33, 1579-1585.

[26] Minoshima, S., Koeppe, R.A., Mintun, M.A., Berger, K.L., Taylor, S.F., Frey, K.A., & Kuhl, D.E. (1993). Automated detection of the intercommissural line for stereotactic localization of functional brain images. *J. Nucl. Med.*, 34, 322-329.

[27] Minoshima, S., Koeppe, R.A., Frey, K.A., & Kuhl, D.E. (1994). Anatomic standardization: linear scaling and nonlinear warping of functional brain images. *J. Nucl. Med.*, 35, 1528-1537.

[28] Zubal, I.G., Harrell, C.R., Smith, E.O., Rattner, Z., Gindi, G., & Hoffer, P.B. (1994). Computerized three-dimensional segmented human anatomy. *Med. Phys.*, 21, 299-302.

[29] Coleman, R.E. (1999). PET in lung cancer. *J. Nucl. Med.*, 40(5), 814-820.

[30] Goerres, G.W., von Schulthess, G.K., & Steinert, H.C. (2004). Why most PET of lung and head-and-neck cancer will be PET/CT. *J. Nucl. Med.*, 45(1), 66S-71S.

[31] Schillaci, O. (2005). Hybrid SPECT/CT: a new era for SPECT imaging? *Eur J. Nucl. Med. Mol. Imaging*, 32, 521–524.

[32] Judenhofer, M.S., Catana, C., Swann, B.K., Siegel, S.B., Jung, W-I, Nutt, R.E., Cherry, S.R., Claussen, C.D., & Pichler, B.J. (2007). PET/MR images acquired with

a compact MR-compatible PET detector in a 7-T magnet. *Radiology*, 224, 807-814.

[33] Hu, S., Hoffman, E.A., & Reinhardt, J.M. (1991). Automated lung segmentation for accurate quantitation of volumetric X-Ray CT images. *IEEE Trans. Med. Imag*., 20(6), 490-498.

[34] Kim, J., Wen, L., Eberl, S., Fulton, R., & Feng, D. (2007). Use of anatomical priors in the segmentation of PET lung tumor images. *Int. Conf. IEEE Med. Imag.*, 6, 4242-4245.

[35] Zijdenbos, P., Dawant, B.M., Margolin, R.A., & Palmer, A.C. (1994). Morphometric analysis of white matter lesions in MR images: Methods and validation. *IEEE Trans. Med. Imag*., 13, 716-724.

[36] Chan, C., Kim, J., Feng, D., & Cai, W. (2005). Interactive fusion and contrast enhancement for whole body PET-CT data using multi-image pixel composting. *Int. Conf. IEEE Med. Imag.,* 2618-2621.

[37] Viola, I., Kanitsar, A., Gröller, M.E. (2005). Importance-driven feature enhancement in volume visualization. *IEEE Trans. Vis. Comput. Graph.*, 11(4), 408-418.

[38] Huang, S-C. (2000). Anatomy of SUV. *Nucl. Med. Biol.,* 27, 643-646.

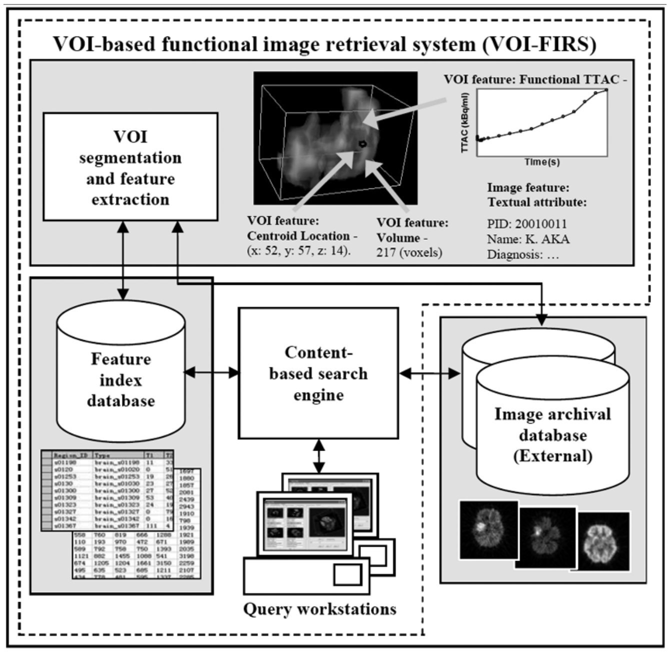

Fig. 1. A System block diagram of CBIR system for dynamic PET images [7]. After VOI segmentation, visual and functional features were extracted and then indexed in the feature index database (feature extraction exemplified using a sample segmented VOI). Workstations were used to query the content-based search engine which retrieves the images stored in the external image archival database.

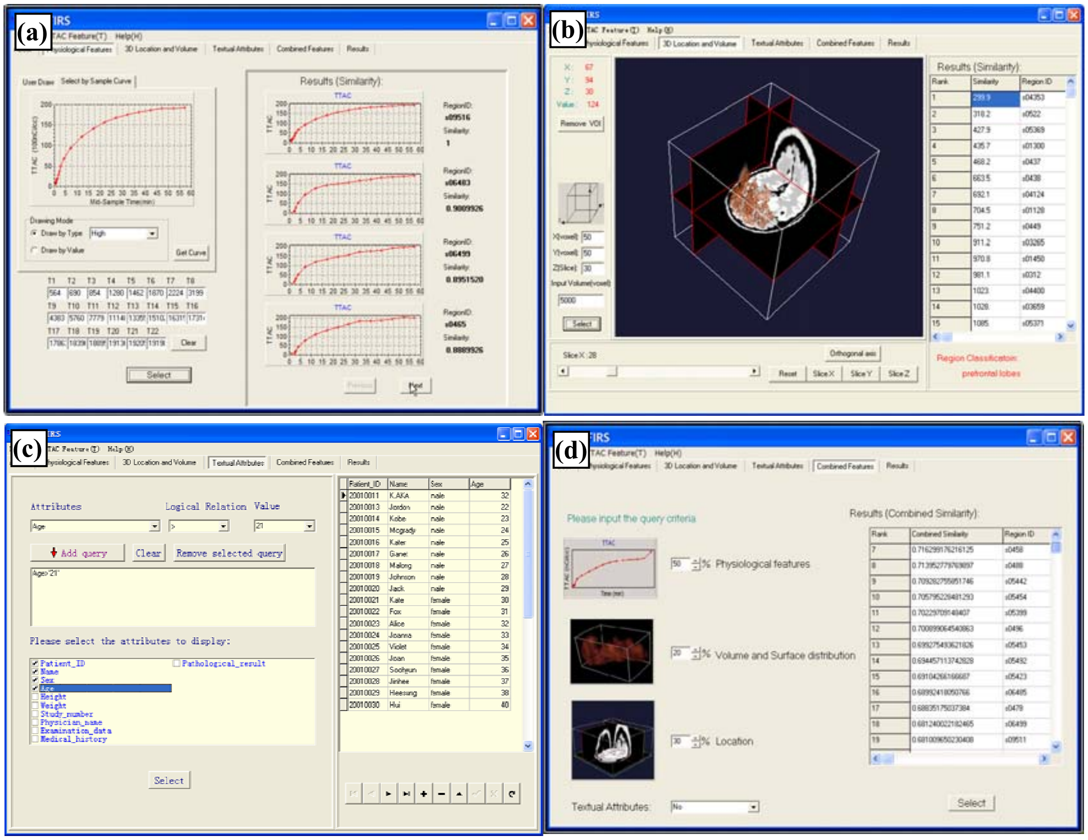

Fig. 2. Four query windows used in the selection of multi-dimensional features [7]. (a) is the “Query by functional and physiological features” interface which shows the user-drawn TTAC curve (left) and the retrieved VOIs with their TTAC curves and similarity indices (right); (b) is the “Query by visual features” interface, exemplified with the rendered surface corresponding to the user-selected “prefrontal lobes” in the orthogonal Zubal slices. (c) is the “Query by textual attribute features” with sample patient selection, and (d) is the “Query by combined features” interface. In all interfaces, left side is the input query and the right side is the retrieved results and its similarity measures.

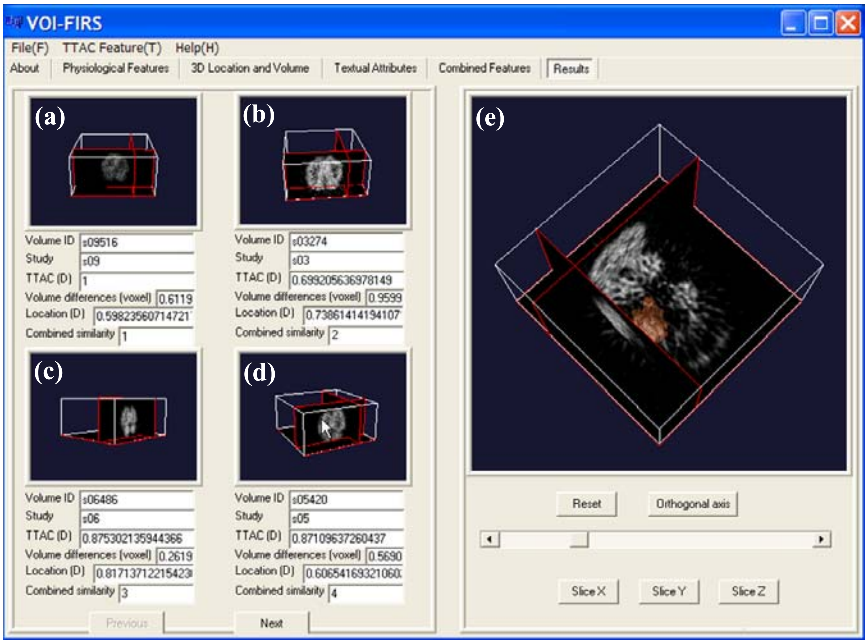

Fig. 3. Thumbnails in the left side of the interface represent the ranked results, respectively of (a) to (d). Right side (e) is the enlarged view of the selected thumbnail result with the retrieved VOI (a tumor structure) surface rendered.

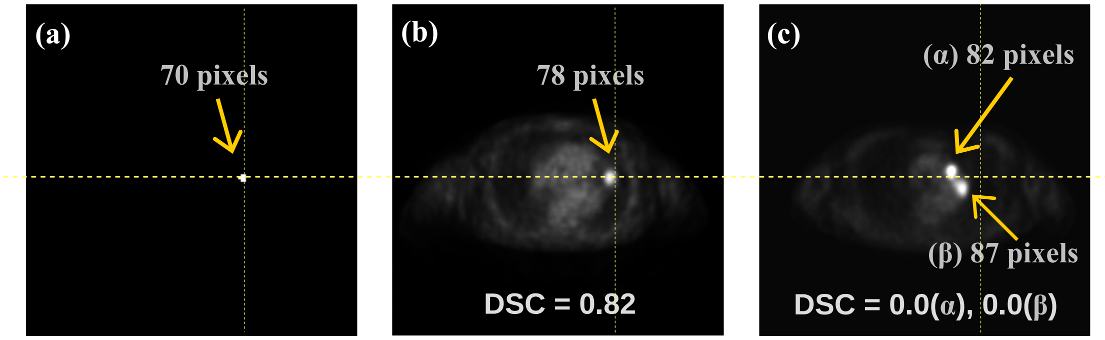

Fig. 4. (a) User-defined query ROI consisting of 70 pixels; (b) and (c) are the retrieved PET images, with with its dice similarity coefficient (DSC) measure again the region in (a).

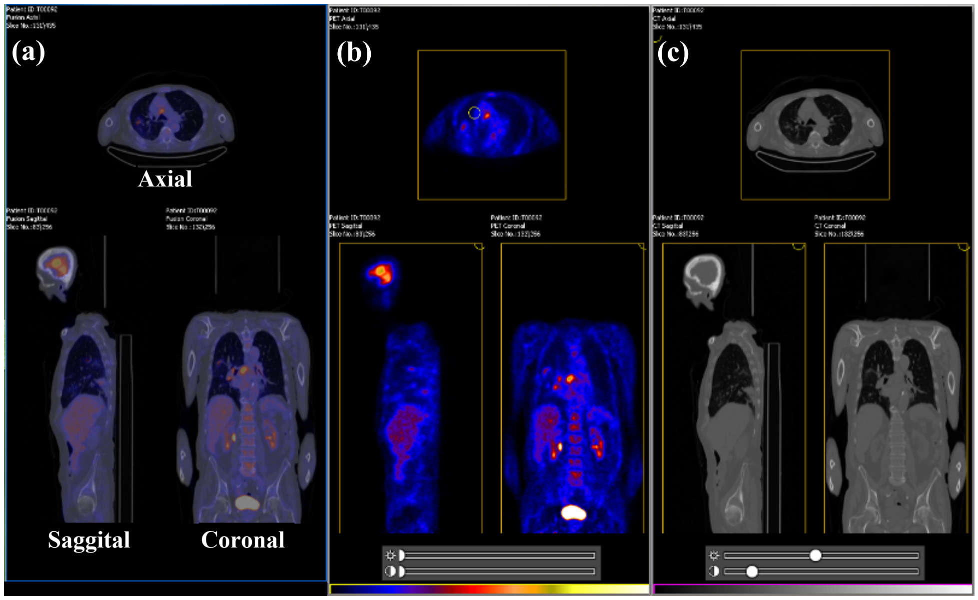

Fig. 5. The retrieved results are presented in a dual-modal PET/CT volumetric viewer that enables interactive user navigation [16]. (a) fused PET/CT with equal fusion ratio; (b) functional PET with multiple tumors indicated by an arrow; and (c) co-aligned anatomical CT. Using the query results, all three orthogonal views were preset to slices that visualize the lung and tumor regions, as exemplified in this figure. Furthermore, image properties such as brightness/contrast and fusion ratio can also be automatically set based on the retrieved slice location. Grayscale LUT was applied for the CT and STD-GAMMA was applied for the PET.